

Altered N-glycan profile of IgG-depleted serum proteins in Hashimoto's thyroiditis

Marta Ząbczyńska^a, Paweł Link-Lenczowski^b, Mislav Novokmet^c, Tiphaine Martin^{d,e},
Renata Turek-Jabrocka^f, Małgorzata Trofimiuk-Müldner^f, Ewa Pocheć^{a,*}

^a Department of Glycoconjugate Biochemistry, Institute of Zoology and Biomedical Research, Faculty of Biology, Jagiellonian University, Gronostajowa 9, 30-387 Kraków, Poland

^b Department of Medical Physiology, Jagiellonian University Medical College, Michałowskiego 12, 31-126 Kraków, Poland

^c Glycoscience Research Laboratory, Genos Ltd., Borongajska cesta 83h, 10000 Zagreb, Croatia

^d Tisch Institute, Icahn School of Medicine at Mount Sinai, 10029 New York, NY, USA

^e Department of Oncological Sciences, Icahn School of Medicine at Mount Sinai, 10029 New York, NY, USA

^f Department of Endocrinology, Jagiellonian University Hospital, Kopernika 17, 31-501 Kraków, Poland

ARTICLE INFO

Keywords:

IgG-depleted serum
N-glycosylation
Sialylation
Hashimoto's thyroiditis
NP-HPLC

ABSTRACT

Background: Hashimoto's thyroiditis (HT) is an autoimmune disease characterized by chronic inflammation of thyroid gland. Although HT is the most common cause of hypothyroidism, the pathogenesis of this disease is not fully understood. Glycosylation of serum proteins was examined in HT only to a limited extent. The study was designed to determine the glycosylation pattern of IgG-depleted sera from HT patients.

Methods: Serum N-glycans released by N-glycosidase F (PNGase F) digestion were analyzed by normal-phase high-performance liquid chromatography (NP-HPLC). N-glycan structures in each collected HPLC fraction were determined by liquid chromatography-mass spectrometry (LC-MS) and exoglycosidase digestion. Fucosylation and sialylation was also analyzed by lectin blotting.

Results: The results showed an increase of monosialylated tri-antennary structure (A3G3S1) and disialylated diantennary N-glycan with antennary fucose (FA2G2S2). Subsequently, we analyzed the serum N-glycan profile by lectin blotting using lectins specific for fucose and sialic acid. We found a significant decrease of *Lens culinaris* agglutinin (LCA) staining in HT samples, which resulted from the reduction of α 1,6-linked core fucose in HT serum. We also observed an increase of *Maackia amurensis* II lectin (MAL-II) reaction in HT due to the elevated level of α 2,3-sialylation in HT sera.

Conclusions: The detected alterations of serum protein sialylation might be caused by chronic inflammation in HT. The obtained results complete our previous IgG N-glycosylation analysis in autoimmune thyroid patients and show that the altered N-glycosylation of serum proteins is characteristic for autoimmunity process in HT.

General Significance

Thyroid autoimmunity is accompanied by changes of serum protein sialylation.

1. Introduction

Hashimoto's thyroiditis (HT) belongs to autoimmune thyroid diseases (AITD), the group of the organ-specific autoimmune disorders characterized by lymphocytic infiltration of the thyroid tissue [1]. Most

of HT patients produce antibodies against thyroid antigens, mainly thyroid peroxidase (TPO) and thyroglobulin (Tg). Anti-thyroid antibodies mediate an immune response which leads to tissue damage. Except for an imbalanced iodide intake, HT is the most common cause of hypothyroidism [2]. There are genetic and environmental

Abbreviations: AITD, autoimmune thyroid diseases; HT, Hashimoto's thyroiditis; LC-MS, liquid chromatography-mass spectrometry; NP-HPLC, normal-phase high performance liquid chromatography; SA, sialic acid; TPO, thyroid peroxidase; Tg, thyroglobulin

* Corresponding author at: Department of Glycoconjugate Biochemistry, Institute of Zoology and Biomedical Research, Jagiellonian University, Gronostajowa 9, 30-387 Kraków, Poland.

E-mail addresses: marta.zabczynska@doctoral.uj.edu.pl (M. Ząbczyńska), p.link-lenczowski@uj.edu.pl (P. Link-Lenczowski), mnovokmet@genos.hr (M. Novokmet), tiphaine.martin@mssm.edu (T. Martin), rjabrocka@gmail.com (R. Turek-Jabrocka), malgorzata.trofimiuk@uj.edu.pl (M. Trofimiuk-Müldner), ewa.pochec@uj.edu.pl (E. Pocheć).

<https://doi.org/10.1016/j.bbagen.2019.129464>

Received 16 July 2019; Received in revised form 9 October 2019; Accepted 15 October 2019

Available online 26 October 2019

0304-4165/ © 2019 The Authors. Published by Elsevier B.V. This is an open access article under the CC BY-NC-ND license (<http://creativecommons.org/licenses/by-nc-nd/4.0/>).

Table 1
List of lectins specific to sialylated and fucosylated glycans used in lectin blotting.

Name	Abbreviation	Sugar specificity	Blocking solution	Vector, Cat. No.
<i>Aleuria aurantia</i> lectin	AAL	Fuc α 1,6-linked to GlcNAc Fuc α 1,3-linked to LacNAc	0.5 M L-Fuc	B-1395
<i>Lens culinaris</i> agglutinin	LCA	Fuc α 1,6-linked to GlcNAc	–	B-1045
<i>Ulex europaeus</i> agglutinin I	UEA-I	α -linked Fuc	0.5 M L-Fuc	B-1065
<i>Maackia amurensis</i> lectin II	MAL-II	α 2,3-linked SA	–	B-1265
<i>Sambucus nigra</i> agglutinin	SNA	α 2,6-linked SA	1 M acetic acid	B-1305

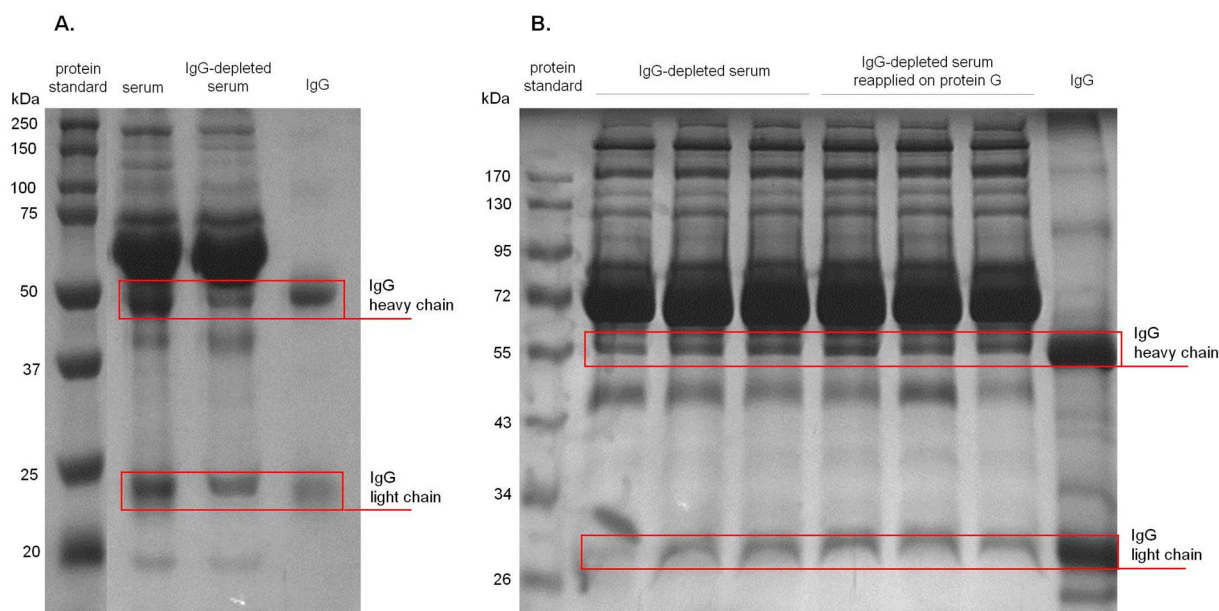


Fig. 1. The efficiency of IgG depletion from human serum using Protein G Spin Plate (Thermo Scientific, 45-204). (A) Representative CBB profile of proteins in whole serum, IgG-depleted serum and purified IgG. (B) The intensity of both IgG chains was not change after reapplication of IgG-depleted serum on Protein G Spin Plate. Serum (10 μ g) and IgG (1 μ g) samples were resolved by 10% SDS-PAGE under reducing conditions. Molecular masses of IgG heavy and light chains were verified using (A) Precision Plus Protein™ Dual Color Standards (Bio-Rad, 1-610-374) and (B) Page Ruler Prestained Protein Ladder (Thermo Scientific, 26-616).

susceptibility factors for HT. Several genes related to immune response together with the gene encoding Tg have been reported as genetic factors associated with HT [1,3]. Infections, allergy, smoking, toxins, and irradiation belong to its environmental factors [4]. It is assumed that loss of self-tolerance characteristic for autoimmune diseases is a result of a dysregulated balance between the activity of Th17 and Th10 lymphocytes [5], which was also reported for AITD [6].

N-glycosylation is a common posttranslational protein modification. During the *N*-glycan synthesis, the oligosaccharide precursor is further modified by the action of several glycosidases and glycosyltransferases. The composition of oligosaccharides, type of linkages between monomers, and a number of branching are the source of the variety of *N*-glycan structures, which belong to three basic groups: high-mannose/oligomannose, hybrid and complex structures. Common *N*-glycan modifications include the addition of sialic acid (SA) at the terminal position of oligosaccharide chain, named sialylation and an attachment of fucose (Fuc) both to the core structure and antennas in the outer part of *N*-glycans, known as fucosylation [7,8].

Human serum *N*-glycoproteome consists of proteins secreted by all body tissues, but its primary sources are liver and plasma cells. The most abundant human serum glycoproteins are immunoglobulins (Ig), transferrin, and α 2-macroglobulin. *N*-glycans play a significant role in the modulation of properties and functions of serum glycoproteins. The oligosaccharide part can modify solubility, half-life time, and conformation of proteins as well as their mutual interactions [9]. Over the last two decades, the serum *N*-glycome analysis became a popular object of interest in search of new disease biomarkers. Changes of serum *N*-glycan profile have been demonstrated mainly in cancers [10–12]

and inflammatory disorders [13]. *N*-glycosylation alterations in chronic inflammation, including autoimmune diseases, have been reported for several serum proteins. Among them, *N*-glycosylation of IgG was shown to be the valuable indicator of rheumatoid arthritis (RA) [14], systemic lupus erythematosus (SLE) [15] and inflammatory bowel disease (IBD) [16]. The reduced galactosylation of IgG in RA is the best-characterized serum glycomarker [17]. Among less abundant serum glycoproteins, inflammation-related changes of *N*-glycosylation were shown for α 1-acid glycoprotein (AGP) and α 2-macroglobulin. The increased level of di- and tetra-antennary structures and the elevated monofucosylation of di- and tri-antennary *N*-glycans on AGP were observed in chronic inflammation [18]. The content of mannose (Man) and galactose (Gal) was significantly higher on α 2-macroglobulin purified from serum samples of SLE patients in comparison to healthy donors [19]. It was shown that a change in glycosylation of a single protein in inflammatory conditions is a result of global serum *N*-glycome rearrangements [20,21]. Many studies have demonstrated that the detection of disease-related glycan changes is also possible at the level of whole serum *N*-glycome analysis. Liquid chromatography-mass spectrometry (LC-MS) analysis of *N*-glycans released from whole serum proteins showed the decrease of fucosylated mono-galactosylated diantennary structures and the increase of tri-antennary galactosylated glycans in RA female patients compared with healthy control [22]. In Crohn's disease (CD) and ulcerative colitis (UC), two chronic IBDs, the total plasma *N*-glycome was also shown to be changed. The decrease of galactosylation accompanied by the enhanced sialylation of diantennary fucosylated structures and α 2,3-sialylation of tri-antennary fucosylated structures was observed in CD. The reduced fucosylation of

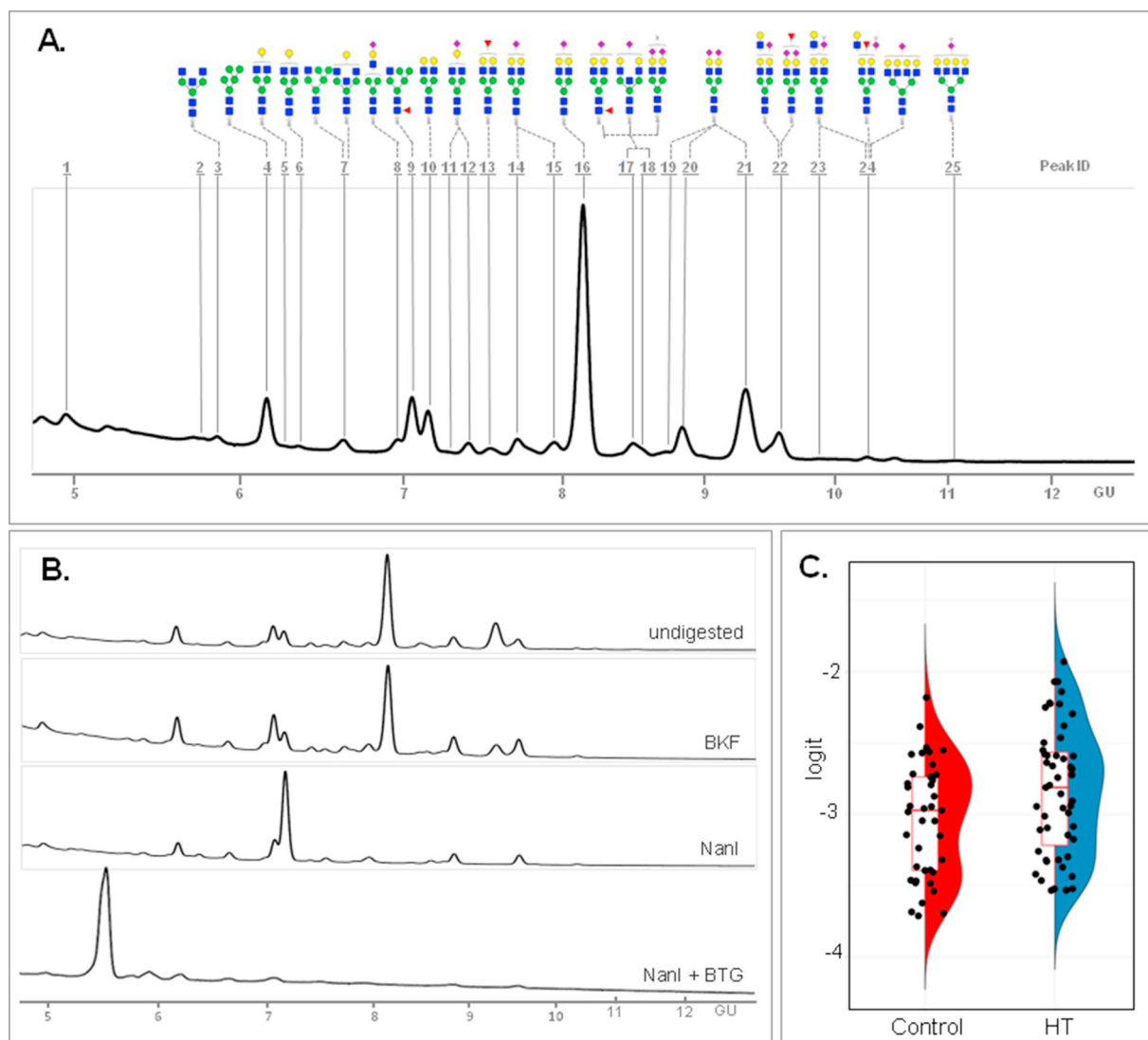


Fig. 2. NP-HPLC analysis of 2-AB-labeled *N*-oligosaccharides released from serum glycoproteins of Hashimoto's thyroiditis patients. (A) The representative chromatogram is showing the separation of the *N*-glycome into 25 individual peaks (peak ID). Schematic structure representations were prepared using GlycoWorkbench; red triangle, fucose; yellow circle, galactose; green circle, mannose; blue square, *N*-acetylglucosamine; purple diamond, sialic acid. (B) The effect of glycan digestion with bovine kidney α 1-2,4,6 fucosidase (BKF), *Clostridium perfringens* α 2-3,6,8 neuraminidase (NanI) and bovine testes β 1-3,4 galactosidase (BTG). (C) The comparison of relative glycan content of peak 22 between control and HT samples showing statistically significant upregulation of glycans in HT ($p = .048$). For statistical analysis, the data were logit-transformed, and the Wilcoxon rank sum (Mann Whitney U) test was applied between the control group and HT group ($p \leq .05$ was considered as statistically significant).

diantennary structures was detected in serum proteins from UC patients. In both IBDs, the higher serum protein sialylation was found [23]. The altered serum or plasma *N*-glycome has been proven for chronic diseases such as schizophrenia [24], chronic hepatitis [25], and numerous types of cancer [12,26,27].

Our recent study showed for the first time a decreased IgG core fucosylation in AITD patients compared to healthy volunteers and the correlation of the reduced fucosylation with serum anti-TPO titer. We also observed lower terminal fucosylation of the peripheral blood mononuclear cells (PBMCs) in HT patients (Martin et al., unpublished data). Our current studies on *N*-glycoproteins in HT IgG-depleted sera are the continuation of the previous research focused on IgG *N*-glycans. We used the sera after IgG depletion to enhance the signal from the less abundant serum *N*-glycoproteins. The study aimed to characterize the protein *N*-glycome of IgG-depleted serum samples from HT patients and assess its potential changes in relation to healthy control. The comparative analysis of serum *N*-glycosylation was performed by lectin profiling of SDS-PAGE separated glycoproteins and normal-phase high-

performance liquid chromatography (NP-HPLC). The detailed *N*-glycan structures were identified using LC-MS/MS.









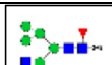
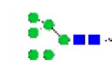





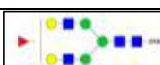




2. Materials and methods

2.1. Study population

51 Hashimoto's thyroiditis female patients (mean age 36.4 ± 12.8) and 41 sex-matched healthy volunteers (mean age 31.9 ± 8.7) were recruited to the study based on medical history, serum level of TSH, anti-TPO, anti-Tg, and thyroid ultrasonography. The groups were age-matched, and no significant difference in age between them was identified (P -value $> .05$). Blood samples were collected between May 2014 and July 2015 at the Endocrinology Clinic of the University Hospital in Krakow. Subjects with other autoimmune diseases, other thyroid diseases, and pregnant women were excluded. The study was approved by the Bioethics Committee of the Jagiellonian University. Informed written consent was given by all study participants.

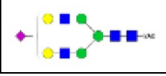

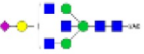
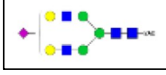
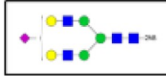
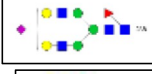
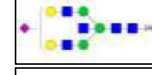
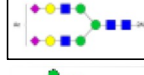
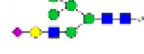
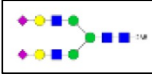
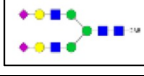
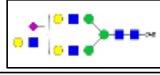
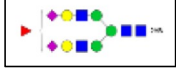
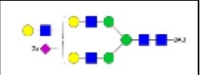
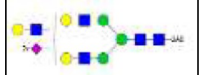
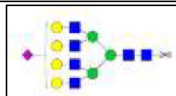
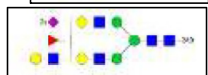
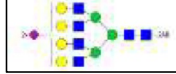
Table 2

List of the most abundant glycan compositions detected in each HPLC fraction. Glycan structural features are proposed based on GU values compared with GlycoStore database and on mass spectrometry (m/z values, complemented by MS2 data where applicable). The structures recognized as the major composition in each glycan peak (GP) are framed. Schematic structure representations were prepared using GlycoWorkbench; red triangle, fucose; yellow circle, galactose; green circle, mannose; blue square, *N*-acetylglucosamine; purple diamond, sialic acid. The abbreviations to the second column: Ac, acetylation; F, fucose; GA, glucuronic acid; H, hexose; N, HexNac. The abbreviations to the fourth column: A1-4, number of antennae; B, bisecting *N*-acetylglucosamine; F, fucose; G, galactose; M, mannose; S, sialic acid.

GP	Composition	Mono mass unlabelled	Proposed glycan structural features	Glycan structure (CFG notation)	Comment
3	H3N5	1519.538	A2B		major composition
4	H5N2	1234.430	M5		major composition
5	H4N4	1478.526	A2G1		major composition
	H4N3F1	1421.508	A1G1F1		significant abundance
6	H4N4	1478.538	A2G1		major composition
7	H5N3	1437.511	M5A1		major composition
	H4N5	1681.614	A2BG1		major composition
8	H4N3S1	1566.523	A1G1S1		major composition
	H6N2	1396.459	M6		minor abundance
	H5N4	1640.558	A2G2		minor abundance
	H4N4S1	1769.593	A2G1S1		minor abundance
9	H5N3F1	1583.542	FM5A1		major composition
	H6N2	1396.461	M6		significant abundance
	H5N4	1640.561	A2G2		significant abundance
	H5N4S1Ac1	1973.659	A2G2S1Ac1		significant abundance
10	H5N4	1640.568	A2G2		major composition
	H4N3	1275.443	A1G1/M4A1		minor abundance
	H5N4S1Ac1	1973.665	A2G2S1Ac1		minor abundance
11/12	H4N4S1	1769.610	A2G1S1		major composition
	H5N4S1Ac1	1973.665	A2G2S1Ac		significant abundance
	H4N3S1 H5N5	1712.588 1843.645	A1G1S1 A2BG2		minor abundance minor abundance
13	H5N4F1	1786.621	A2F1G2 FA2G2		major composition
	H6N3	1599.539	M5A1G1		significant abundance
	H5N4S1	1931.646	A2G2S1		significant abundance
	H5N4S1Ac	1973.663	A2G2S1Ac		significant abundance
	H4N4S1	1769.606	A2G1S1		minor abundance

(continued on next page)

Table 2 (continued)

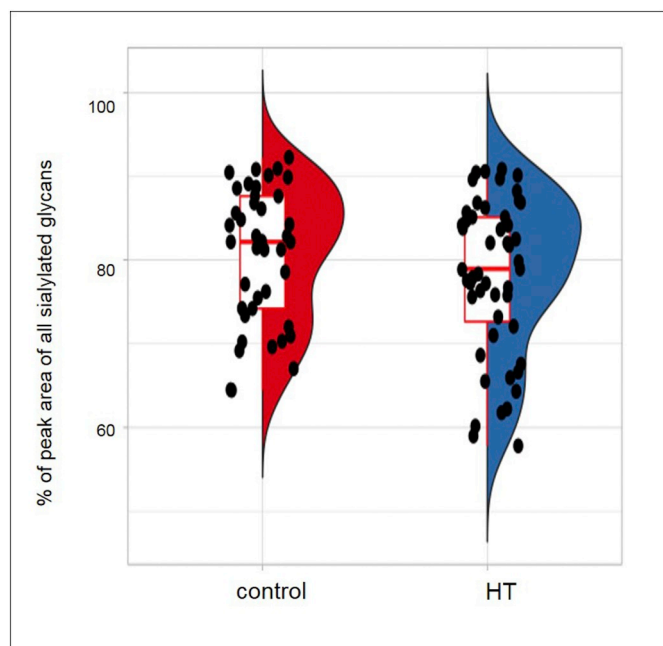
14	H5N4S1	1931.658	A2G2S1		major composition
	H5N3S1	1728.582	M4A1G1S1		significant abundance
	H4N5S1	1972.675	A2BG1S1		significant abundance
15	H5N4S1	1931.653	A2G2S1		major composition
	H4N5S1	1972.673	A2BG1S1		minor abundance
16	H5N4S1	1931.644	A2G2S1		major composition
17/18	H5N4F1S1	2077.710	FA2G2S1		major composition
	H5H5S1	2134.729	A2BG2S1		major composition
	H5N4S2Ac1	2264.750	A2G2S2Ac1		major composition
	H6N3S1	1890.632	M5A1G1S1		significant abundance
	H6N5	2005.690	A3G3		minor abundance
19/20	H5N4S2	2222.739	A2G2S2		major composition
21	H5N4S2	2222.839	A2G2S2		major composition
	H6N5S1	2296.773	A3G3S1		probably coelution from GP22
22	H6N5S1	2296.773	A3G3S1		major composition
	H5N4F1S2	2368.791	A2F1G2S2		major composition
	H5N4S2	2222.740	A2G2S2		coelution from GP21
23	H6N5S2	2587.863	A3G3S2		major composition
	H5N4S1GA1	2107.671	A2G2S1GA1		minor abundance
	H6N5F1S1	2442.835	A3F1G3S1		minor abundance
24	H6N5S2	2587.865	A3G3S2		major composition (coelution from GP23)
	H7N6S1	2661.901	A4G4S1		major composition
	H6N5F1S2	2733.923	A3F1G3S2		major composition
25	H7N6S2	2952.979	A4G4S2		major composition

2.2. Serum sample collection

Blood was collected via venous puncture into S-Monovette serum tubes (Sarstedt, 05.1557.001). Blood samples were left at room temperature for five hours for blood coagulation and then were centrifuged at $1200 \times g$ for 10 min (Heraeus). Serum samples were stored in deep freezing.

2.3. IgG depletion

Serum was diluted 1:1 with the binding buffer (0.1 M Na_2HPO_4 , 0.15 M NaCl, pH 7.5). 20 μl of each diluted sample was applied to the Protein G Spin Plate (Thermo Scientific, 45-204) and incubated 15 min. at room temperature on the orbital shaker (JW Electronic). Then 20 μl of the binding buffer was added to each well and incubated for the next



Supplementary Fig. 1. The comparative analysis of total sialylation between control group and Hashimoto's thyroiditis patients (HT). The total sialylation was measured as a sum of relative intensities of the HPLC glycan peaks with the annotated sialylated oligosaccharides (GP8,11,12,14-25). For statistical analysis, the data were logit-transformed, and the Wilcoxon rank sum (Mann Whitney U) test was applied between the control group and HT group ($p \leq .05$ was considered as statistically significant).

15 min. After incubation, the plate was centrifuged ($1000 \times g$, 1 min.). The flow-through fraction containing IgG-depleted serum was collected and deeply frozen until the experiment.

2.4. Coomassie brilliant blue staining

The efficiency of IgG depletion from human sera was assessed by Coomassie Brilliant Blue (CBB) staining. Whole serum and IgG-depleted serum proteins (10 μ g), and purified IgG (1 μ g) were resolved by 10% SDS-PAGE under reducing conditions followed by CBB staining (Sigma-Aldrich, B-2025). Molecular masses of IgG heavy and light chains were verified using Precision Plus Protein™ Dual Color Standards (Bio-Rad, 1610374) or Page Ruler Prestained Protein Ladder (Thermo Scientific, 26616).

2.5. Normal-phase high-performance liquid chromatography (NP-HPLC)

2.5.1. PNGase digestion

40 μ l of diluted serum was reduced with 2.5 μ l 200 mM dithiothreitol (DTT, Sigma-Aldrich) and incubated at 60 °C for 45 min. After cooling down to room temperature (RT), 10 μ l of iodoacetamide (IAA, Sigma-Aldrich) was added and incubated in darkness for 1 h in room temperature. Then 2.5 μ l of DTT was added again to serum proteins. Samples were diluted by adding 100 μ l of the binding buffer and 300 μ l of Milli-Q water. Then 100 mU of PNGase F (Sigma-Aldrich, P-7367) was added, and serum glycoproteins were deglycosylated overnight at 37 °C. Following PNGase digestion, 10% trifluoroacetic acid (TFA, Fluka) was added to each sample, and the released N-glycans were cleaned-up using C18 SPE column (Supelco) and subsequently Carbohydrate SPE column (Supelco) according to Biskup et al. (2013) [28]. Purified N-glycans were dried down by lyophilization (Labconco).

2.5.2. 2-AB labeling

Anthranilic acid amide (2-AB) (Sigma-Aldrich) and sodium

cyanoborohydride (Fluka) were dissolved in acetic acid, and DMSO (3:2) mixture and 10 μ l of the labeling solution was added to the dried N-glycans and incubated at 65 °C for 3 h. After cooling down to RT, the excess of labeling solution was removed using Speed SPE Cartridges (Applied Separation), and 2-AB-labeled N-glycans were eluted in Milli-Q water, according to Link-Lenczowski et al. (2018) [29]. Purified N-glycans were dried down by lyophilization and stored at -70 °C before analyses by HPLC and MS.

2.5.3. Exoglycosidase digestion

50 μ l of 2-AB-labeled N-glycans were dried down in SpeedVac centrifuge (Savant) and treated with bovine kidney α 1-2,4,6 fucosidase (BKF), *Clostridium perfringens* α 2-3,6,8 neuraminidase (NanI), and bovine testes β 1-3,4 galactosidase (BTG) (New England Biolabs). The exoglycosidase digestion was performed according to the manufacturer's protocol at 37 °C overnight. To remove enzyme protein from the samples Amicon Ultra 10 K (Millipore) centrifugal filters were used. After cleaning step, digested N-glycans were dried down in SpeedVac concentrator (Savant).

2.5.4. NP-HPLC analysis

2-AB-labeled N-glycans were separated on Tosoh TSK gel-Amide 80 column (4.6×150 mm, 3 μ m bead size) (Tosoh Bioscience, Griesheim, Germany) using Shimadzu Prominence HPLC system (Shimadzu) with RF-20Ax fluorescence detector. Solvent A was acetonitrile (ACN), and solvent B was 50 mM ammonium hydroxide in Milli-Q water, titrated to pH 4.4 with formic acid. The samples were loaded in 70% ACN and the chromatography was performed using high-resolution binary gradient under following conditions: temp = 50 °C; flow rate = 1.25 ml/min; time = 0 min ($t = 0$), 30% B; $t = 30.25$, 48% B; $t = 31$, 100% B; $t = 33$, 100% B; $t = 34$, 30% B; $t = 40$, 30% B. The chromatographic system was under control of Shimadzu LabSolutions 5.90 software. After each set of 10 samples, the external standard (2-AB-labeled glucose oligomer ladder; Glyco Prozyme) was separated. HPLC chromatograms were integrated into 25 glycan peaks. The annotation of glycan peaks was performed basing on mass spectrometry analysis and their glucose units (GU) values compared to GlycoStore database (www.glycostore.org) [30,31]. The percentage area of each peak represents its relative content within the chromatogram.

2.6. Liquid chromatography-mass spectrometry

NP-HPLC peaks were manually fractionated, concentrated by evaporation and reconstituted in 10 μ l of ultrapure water. Liquid chromatography-mass spectrometry (LC-MS) analysis of concentrated NP-HPLC fractions were performed using nanoACQUITY UPLC system from Waters (Waters, Massachusetts, USA) coupled to a Compact mass spectrometer (Bruker Daltonics, Bremen, Germany) as described before [32]. Briefly, the chromatography system consists of a reverse phase trap column (Acclaim PepMap C18, 1 mm \times 300 μ m i.d., Thermo Fisher Scientific) and of an analytical column (Halo C18 nano-LC column; 150 mm \times 75 μ m i.d., 2.7 μ m HALO fused core particles; Advanced Materials technology, USA). The separation was performed using 0.1% formic acid in water as solvent A and 95% acetonitrile as solvent B at the 1 μ l/min flow rate. The LC system was coupled via online capillary electrophoresis (CE) ESI-MS sprayer source (Agilent, California, USA) to a Compact mass spectrometer operated in the positive ion mode. Glycan compositions were assigned using GlycoWorkbench [33] and Glycomode (<http://web.expasy.org/glycomod/>) according to obtained MS and MS/MS spectra.

2.7. Lectin blotting

The set of selected lectins (Vector Lab.) were used to assess serum protein fucosylation and sialylation. The lectins blocked by specific sugars were used as the negative controls (Table 1). Lectin blotting was

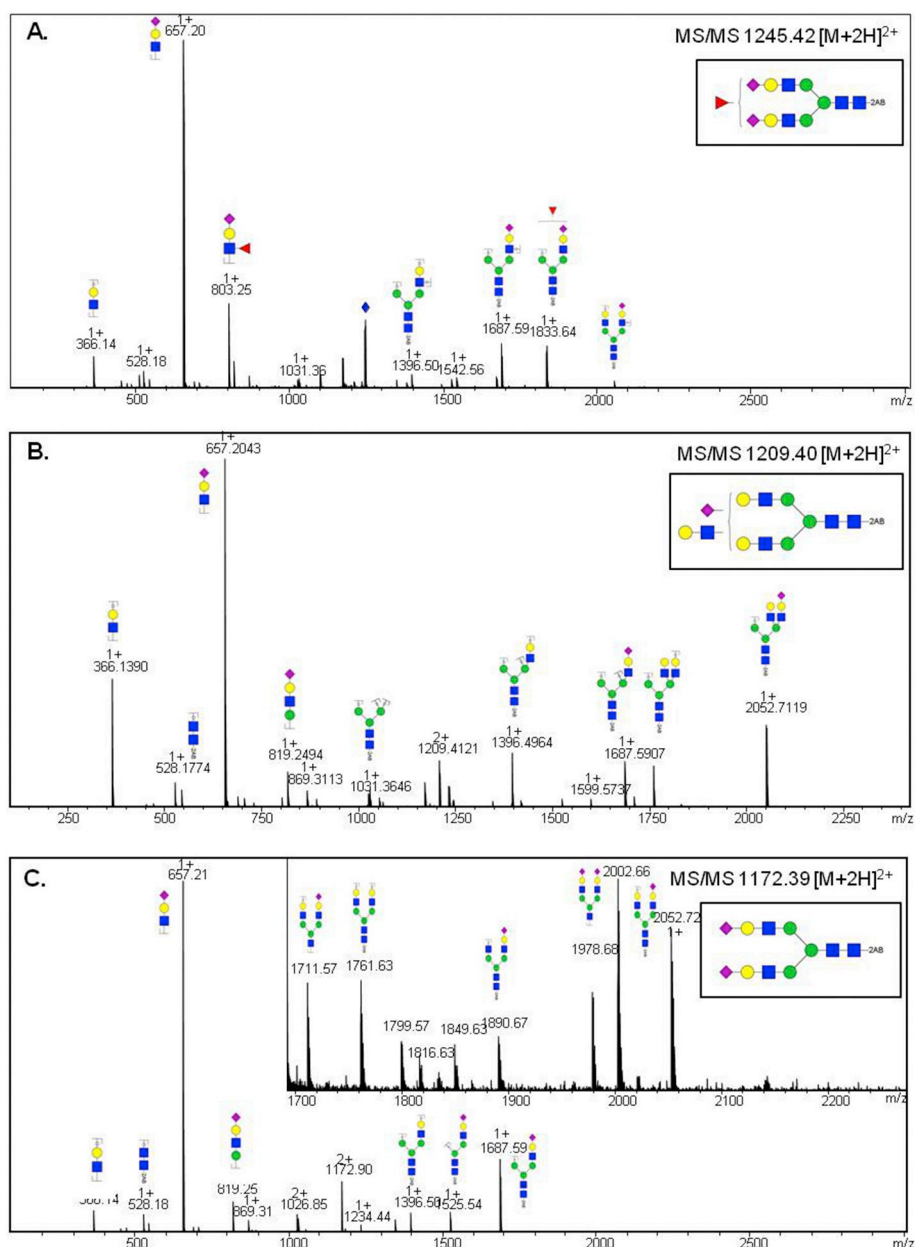
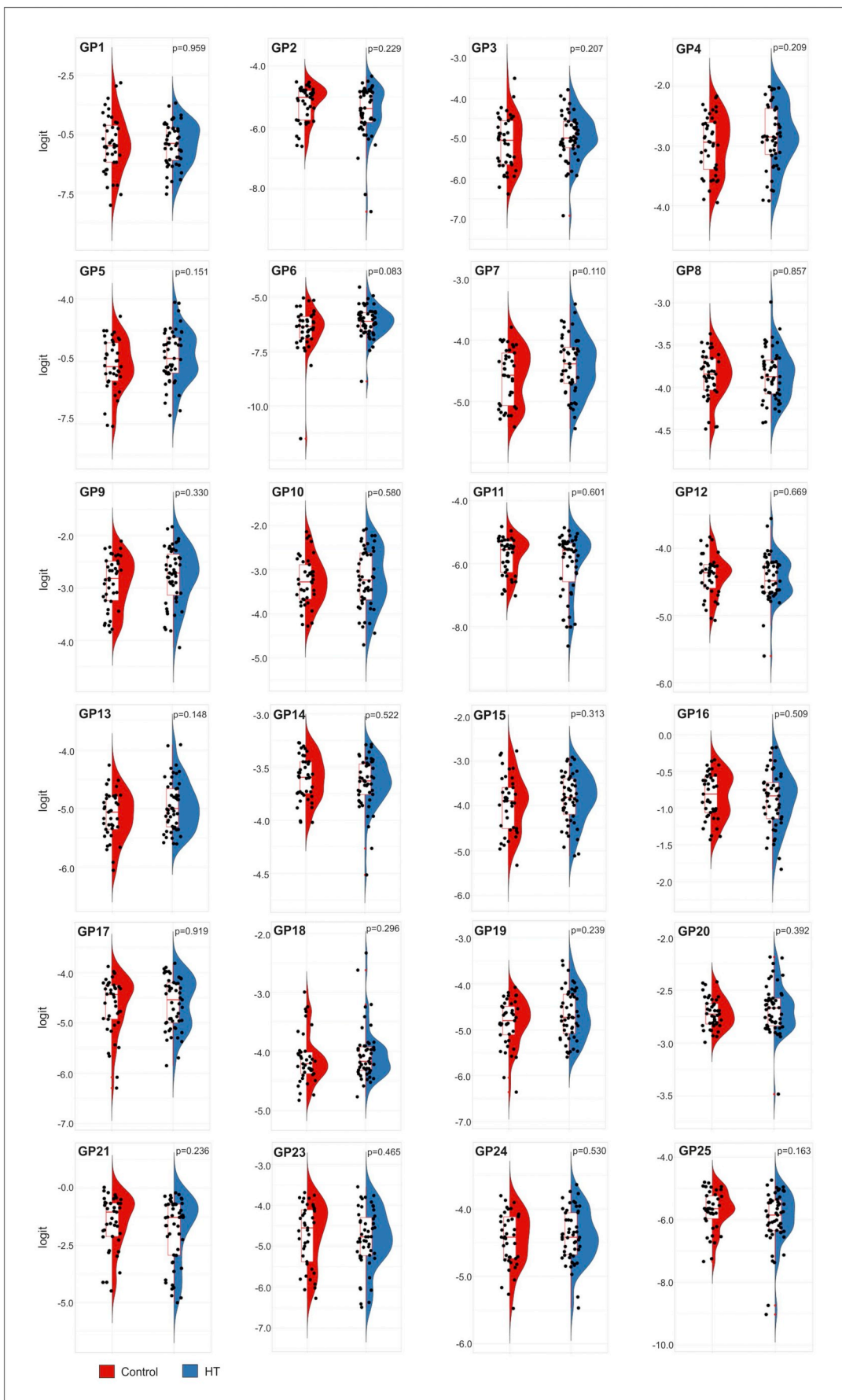


Fig. 3. ESI-MS/MS spectra of precursor ions from peak 22 fraction collected from NP-HPLC. The suggested glycan structures are given in rectangles. The fragment ion at m/z 657.2 in A, B and C is indicative for terminally sialylated antennas, fragment ion at m/z 803.2 clearly indicates the presence of fucosylated antenna in A. Schematic structure representations were prepared using GlycoWorkbench; red triangle, fucose; yellow circle, galactose; green circle, mannose; blue square, *N*-acetylglucosamine; purple diamond, sialic acid.

performed as described by Hoja-Lukowicz et al. (2013) [34]. Briefly, 10 μ g of IgG-depleted serum proteins or whole serum proteins were boiled in Laemmli sample buffer (Bio-Rad Lab.) with 5% β -mercaptoethanol for 5 min. and separated on 10% stain-free gels (Bio-Rad Lab.). The resolved proteins were visualized on gels using Gel Doc EZ Imaging System with Image Lab software (Bio-Rad Lab.). Then the proteins were electroblotted to the PVDF membranes (Millipore), and the blots were blocked overnight using Carbo Free Blocking Solution (Vector Lab.) to avoid nonspecific binding. After washing three times with TBS, the blots were incubated for 1 h with the lectins followed by incubation with alkaline phosphatase-conjugated ExtrAvidin (Sigma-Aldrich, E-2636) for 1 h at RT. Glycoprotein bands were visualized by the colorimetric reaction catalyzed by alkaline phosphatase. The intensity of lectin staining on each lane was measured densitometrically and was normalized to the protein signal on corresponding gel lanes using Image Lab software (Bio-Rad Lab.). The lectin blotting was

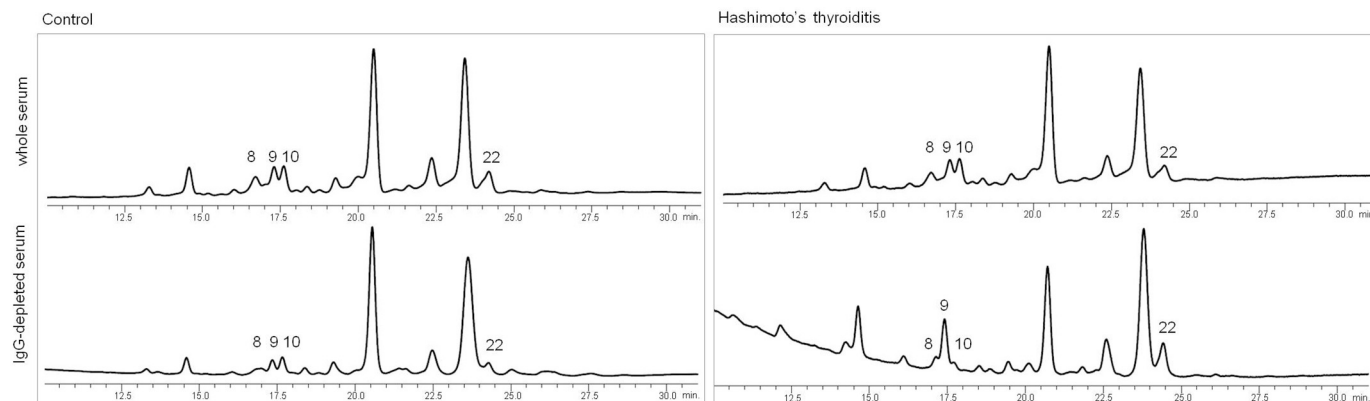
performed in duplicates or triplicates.

To determinate the signal from *O*-glycans we performed PNGase digestion followed by the lectin blotting. IgG-depleted serum (10 μ g) in the phosphate buffer (50 mM Na_2HPO_4 , pH 7.5) was reduced by adding 1 μ l 5% SDS and incubated at 100 $^\circ\text{C}$ for 3 min. After cooling down 1.5 μ l of Nonidet P-40 (Fluka) and 0.5 U of PNGase F (Sigma-Aldrich, P-7367) were added, and incubated overnight at 37 $^\circ\text{C}$. PNGase-digested and untreated serum samples were resolved on 10% SDS-PAGE and destined to lectin blotting. Non-specific lectin reaction was verified by the pre-incubation of lectin with specific sugar (0.5 M fucose for AAL and UEA-I; 0.2 M lactose in 0.4 M acetic acid for SNA) or glycophorin, a protein bearing sialylated glycans (Sigma-Aldrich, G-9511, diluted 1:500 for MAL-II).



(caption on next page)

Supplementary Fig. 2. The comparison of relative glycan content of HPLC peaks (GP1-21, 23-25) between control and Hashimoto's thyroiditis patients (HT). For statistical analysis, the data were logit-transformed, and the Wilcoxon rank sum (Mann Whitney U) test was applied between the control group and HT group ($p \leq .05$ was considered as statistically significant).



Supplementary Fig. 3. Representative HPLC chromatograms of *N*-glycans derived from the whole serum and IgG-depleted serum of healthy donor (control) and Hashimoto's thyroiditis patient. *N*-glycans were enzymatically liberated from serum proteins, 2-AB labeled and analyzed by NP-HPLC with fluorescent detection. Glycans peak indications correspond to the peak ID numbers presented in Fig. 2.

2.8. Statistical analysis

Glycan HPLC data represent the relative percentage areas derived from the chromatogram (% area), with the sum of the values to a constant value at 100% (or 1). First, based on quality control, one sample was discarded. Then we applied a logit transform ($\text{logit}(\text{peak}) = \log(\text{peak}/(1-\text{peak}))$) on different data. A non-parametric statistical hypothesis test, Wilcoxon rank sum (Mann Whitney U) test, was applied between the control group and HT group for each peak of the chromatogram. *P*-values obtained from Mann Whitney U test were FDR-corrected using the method of Benjamini and Hochberg (1995) [35]. Results with an FDR of $< 5\%$ were considered statistically significant whereas results with *P*-value non-adjusted $< 5\%$ were considered statistically nominal significant.

Glycan lectin data represent the intensity of lectin staining measured densitometrically for each line and normalized to the protein signal on the corresponding gel lane. Lectin tests have been performed on different PVDF membranes and batches. Consequently, we analyze the association between lectin value with AITD status using a linear mixed model with age as fixed effect and individual, membrane, and batch as a random effect. *P*-values obtained from the ANOVA test were FDR-corrected using the method of Benjamini and Hochberg (1995) [35]. Results with an FDR of $< 5\%$ were considered statistically significant whereas results with *P*-value non-adjusted $< 5\%$ were considered statistically nominal significant.

3. Results

Depletion of IgG from human serum samples was performed using protein G resin plate. The serum volume was experimentally established to remove IgG efficiently (Fig. 1). CBB profiles showed that majority of IgG was depleted from serum sample (Fig. 1A). After reapplication of IgG-depleted serum on the Protein G Spin Plate (Thermo Scientific) the intensity of protein bands corresponding to both IgG chains was unchanged in CBB profile (Fig. 1B) which suggests that other proteins with similar molecular weight are present in the bands corresponding to IgG heavy and light chains. IgG-depleted sera were destined to the analysis of glycan structure by HPLC, LC-MS and lectin blotting. These methods represent two different analytical approaches to *N*-glycan profiling. HPLC and LC-MS analyze released *N*-glycans while in lectin blotting specific glycoepitopes on SDS-PAGE separated glycoproteins are detected.

NP-HPLC was performed to compare the *N*-glycan profiles for IgG depleted-sera from HT patients and healthy donors. The obtained chromatograms were manually integrated into 25 separated glycan peaks (GPs). The representative HPLC chromatogram is shown in Fig. 2A. *N*-glycan HPLC pattern was uniform for HT and control samples with predominant GP16 observed at GU 8.15. For the detailed structural analysis, *N*-glycans were fractionated by NP-HPLC according to the retention time of the integrated peaks. Each HPLC fraction was collected and destined to determine *N*-glycan composition by LC-MS. Three pairs of the close located neighboring peaks (GP11/12, GP17/18, and GP19/20) were pooled because it was impossible to separate them during manual collection of the fractions. Table 2 presents *N*-glycans assigned to the GPs, except for GP1 and GP2 with the lowest intensity in NP-HPLC chromatograms. The structures recognized as the major composition in each GP are framed. The majority of *N*-glycans are the complex structures (di- to tetra-antennary) with mono- or disialylated antennae. Five fucosylated *N*-glycans were identified, and among them, three contains antennary Fuc residues.

The relative intensity of each GP was expressed as an area percent (% area) of the total integrated area. For statistical analysis the data were transformed using ($\text{logit}(\text{peak}) = \log(\text{peak}/(1-\text{peak}))$) formula, where peak corresponds to % area. The total sialylation of HT serum proteins measured as a sum of relative intensities of the peaks with the annotated sialylated structures (GP8,11,12,14–25) was reduced in relation to control group, but this change was not statistically nominal significant ($p = .291$) (Supplementary Fig. 1). The comparison of relative intensities for each peak separately showed a statistically significant increase of the GP22 (GU 9.51) abundance in HT samples ($p = .048$) (Fig. 2C). Two major *N*-glycan structures: monosialylated tri-antennary glycan (A3G3S1; m/z 1209.40) and disialylated di-antennary structure with antennary Fuc (FA2G2S2; m/z 1245.42) were identified using LC-MS/MS analysis as the ones contributing to the FLR signal of the GP22. Third structure assigned to GP22 (A2G2S2) was co-eluted from the neighboring fraction of GP21. The LC-MS/MS spectra for *N*-glycans assigned to GP22 are presented in Fig. 3. The two predominant HPLC peaks GP16 and GP21 contain the complex-type di-antennary monosialylated (GP16, A2G2S1) and disialylated (GP21, A2G2S2) *N*-glycan structures. For the rest of HPLC GPs the statistically significant differences were not found (Supplementary Fig. 2).

The HPLC peak annotation was additionally verified by the analysis of the exoglycosidase-digested *N*-glycans. We observed the evident shift of the GP16 and GP21 after treatment with α -2,3,6,8 neuraminidase

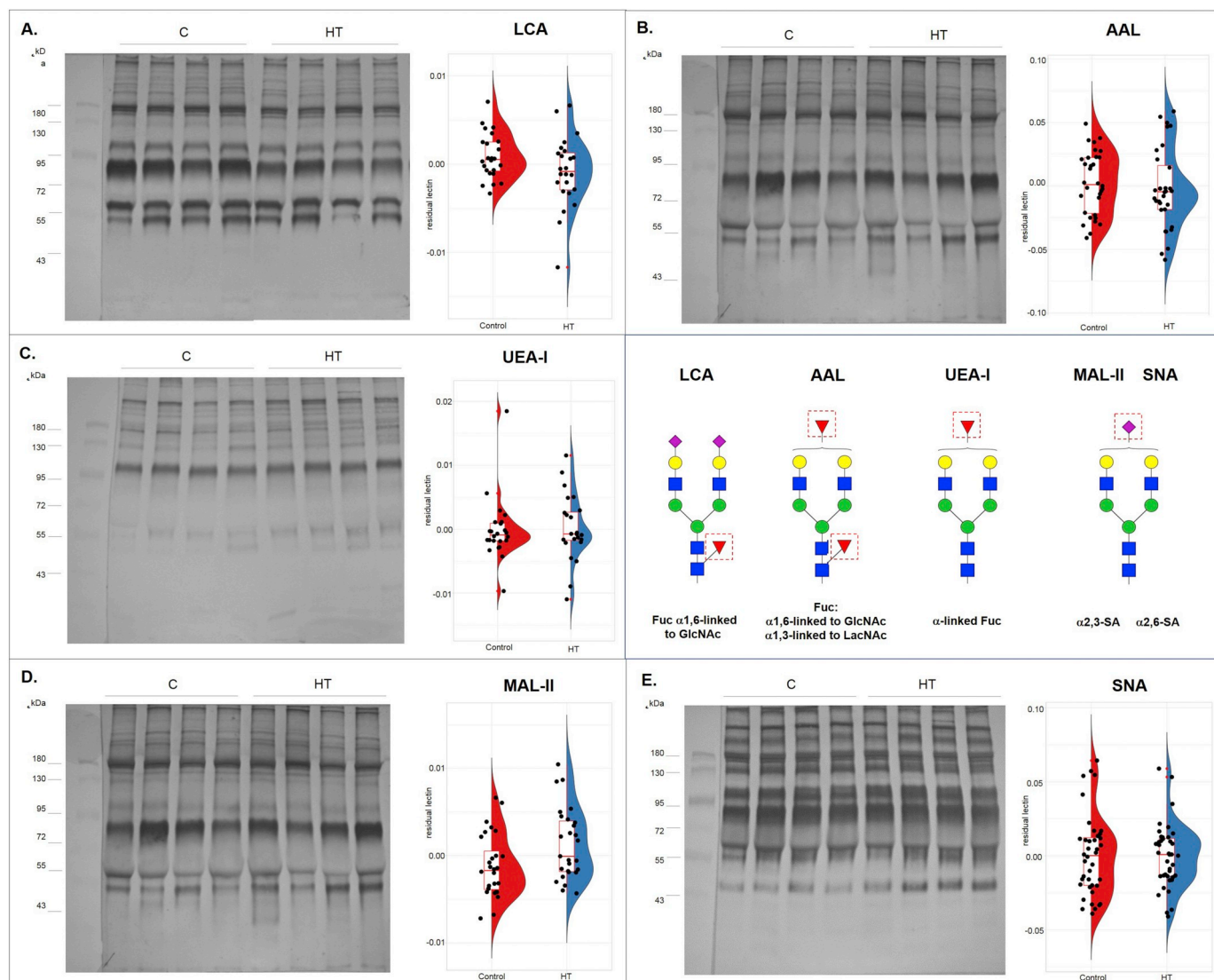


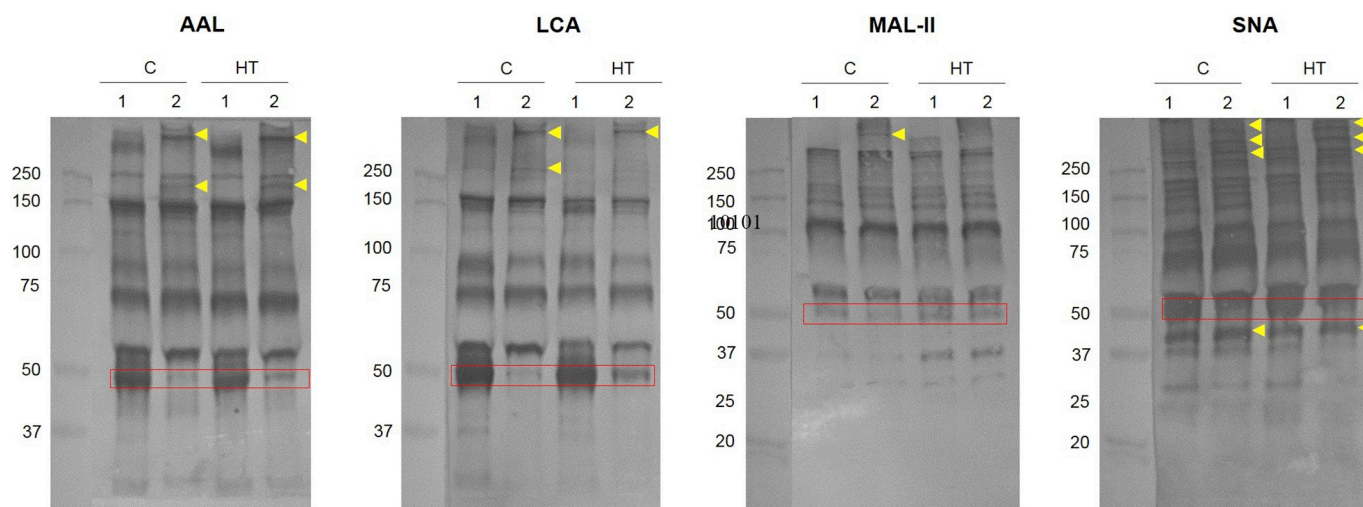
Fig. 4. Lectin analysis of serum glycan fucosylation (A-C) and sialylation (D, E). IgG-depleted serum proteins from healthy individuals (C, $n = 20$) and Hashimoto's thyroiditis patients (HT, $n = 20$) separated on stain-free gels, were incubated with the lectins specific for fucose (LCA, AAL, UEA-I) and sialic acid (MAL-II, SNA). Fucosylated and sialylated glycoproteins were visualized colorimetrically. Molecular masses were verified using Precision Page Ruler Prestained Protein Ladder (Thermo Scientific, 26616). The intensity of lectin staining on each lane was measured densitometrically and was normalized to the protein signal on corresponding gel lanes. P -values from the ANOVA test were FDR-corrected and the results with an FDR of $< 5\%$ were considered statistically significant ($p = .042$ for LCA, $p = .031$ for MAL-II). Schematic structure representations were prepared using GlycoWorkbench; red triangle, fucose; yellow circle, galactose; green circle, mannose; blue square, N -acetylglucosamine; purple diamond, sialic acid.

(NanI). The intensity of GP16 was not changed and GP21 was partially reduced when α 1-2,4,6 fucosidase (BKF) was applied. In the case of GP22, the effect of NanI and BKF was not as clearly visible due to the overlapping of peaks being the products of digested GP23-GP25. This was confirmed when β 1-3,4 galactosidase (BTG) together with the sialidase was applied (Fig. 2B).

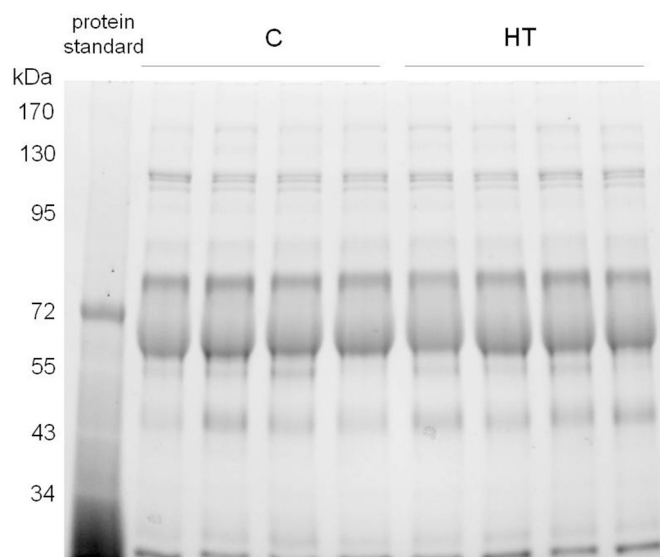
N -glycans liberated from whole serum proteins and IgG-depleted serum proteins were also compared (Supplementary Fig. 3). The chromatographic profiles of both sample types are similar suggesting that no evident qualitative differences are present. However, some qualitative variations between the whole serum and IgG-depleted serum glycomes were observed, particularly in case of GP8-10. Additionally, a slightly different retention time of GP22 in the profiles of whole serum and IgG-depleted serum was found. It would indicate that in this retention time area the N -glycans from both samples separate slightly differently. Taking into account also the quantitative differences in GP22 between control and HT samples (Fig. 2C), looking for glycosylation changes in IgG-depleted serum seems to be reasonable. Otherwise, these

differences could be masked by IgG-derived glycans.

Complementary to HPLC, the lectin blotting analysis was performed using set of biotinylated lectins specific for SA and Fuc residues (Fig. 4). Comparative lectin staining of the whole serum and IgG-depleted serum proteins showed a significantly or completely reduced intensity of bands corresponding to IgG heavy and light chains (Supplementary Fig. 4) which confirmed that IgG was efficiently removed from serum. The profile of SDS-PAGE-resolved serum proteins was quantitatively comparable for C and HT samples (Supplementary Fig. 5). To standardize data, obtained in each experiment and on each PVDF membrane, the values from the densitometric analysis were transformed using the model described in Materials and methods, and the ANOVA test was performed. The lectin staining revealed the differences in the intensity of single protein bands between the IgG-depleted serum samples (Fig. 4). However, they were specific for individual donors. The sialylation and fucosylation of serum proteins were compared between control and study groups by measuring the intensity of the lectin reaction with all separated glycoproteins for one sample normalized to



Supplementary Fig. 4. Lectin blotting of the whole sera (1) and IgG-depleted sera (2) from healthy donors (C, control) and Hashimoto's thyroiditis patients (HT). Serum samples (10 μ g) were separated by 10% SDS-PAGE under reducing conditions. Molecular masses of IgG heavy chains were verified using Precision Plus Protein™ Dual Color Standards (Bio-Rad, 1-610-374). IgG heavy chain is marked in a red frame. The bands corresponding to glycoproteins with the stronger staining in IgG-depleted serum compared to the whole serum were marked by yellow arrowheads.



Supplementary Fig. 5. Protein profile of IgG-depleted sera from healthy donors (C, control) and Hashimoto's thyroiditis patients (HT) obtained using stain-free system (Bio-Rad). IgG-depleted serum proteins (10 μ g) were resolved in 10% SDS-PAGE stain-free gels under reducing conditions. Page Ruler Prestained Protein Ladder (Thermo Scientific, 26-616) was used as the protein standard.

the intensity of proteins measured in stain-free gels. The statistical analysis showed a significant decrease in the densitometric signal for LCA reaction in HT samples ($p = .042$). The weaker LCA staining corresponds to the reduction of the α 1,6-linked core fucosylation in HT serum glycoproteins (Fig. 4A). We also observed the statistically significant increase of MAL-II reaction in HT ($p = .031$), which results from the elevated level of α 2,3-sialylation in HT sera (Fig. 4D). The comparison of AAL, UEA-I, and SNA staining between C and HT samples showed no statistically significant differences with $p = .40$, $p = .83$, $p = .97$, respectively (Fig. 4 B, C, E). In the analysis with fucose-specific lectins we did not observe a signal from PNGase treated samples after reaction with LCA and a weak signal for UEA-I and AAL (Supplementary Fig. 6A). Whereas in case of lectins specific for sialylated glycans we found the positive SNA and MAL-II reaction with PNGase-treated serum proteins, which indicates on the presence of α 2,6- and α 2,3-sialylated *O*-glycans (Supplementary Fig. 6B).

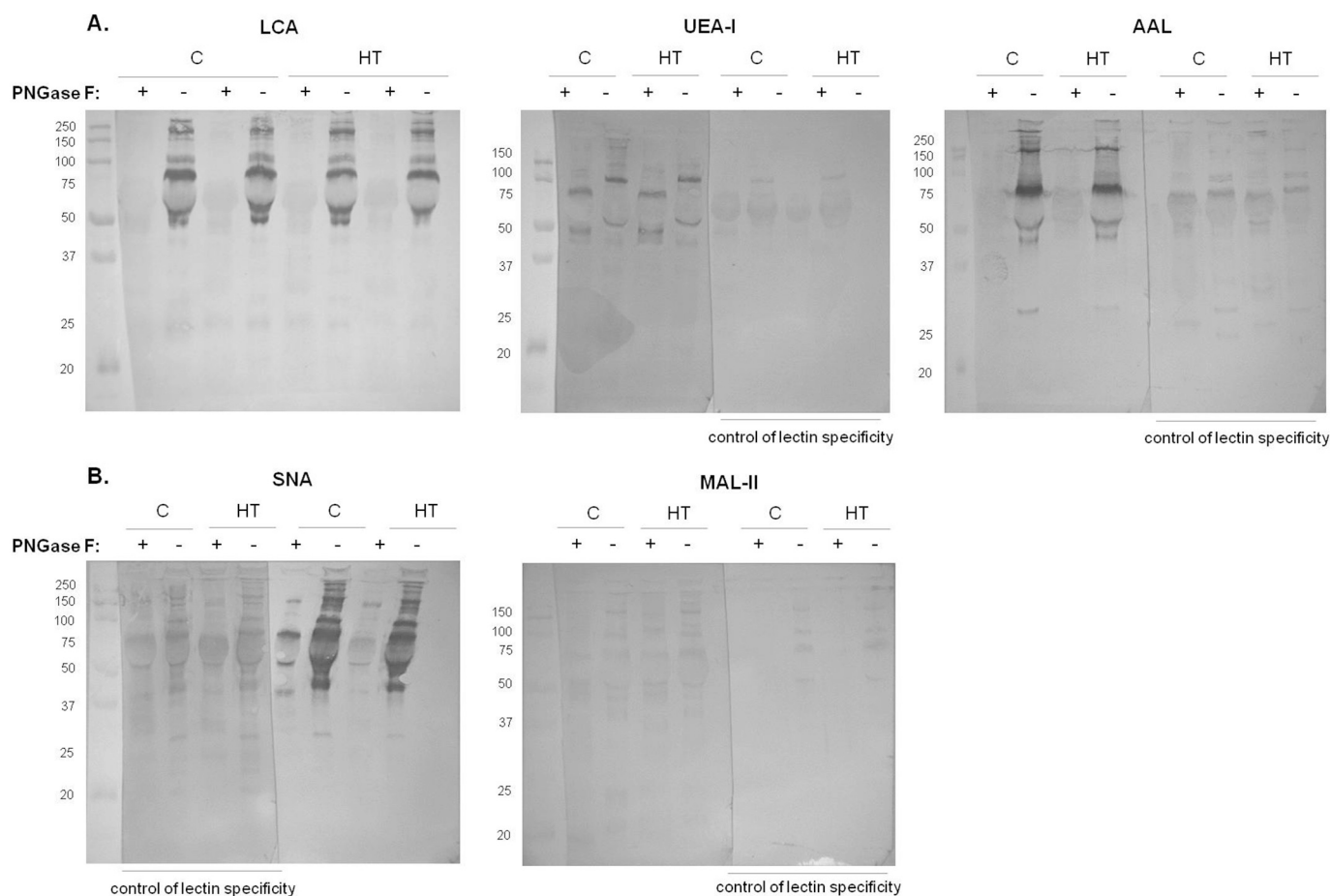
Taken together, the enhanced α 2,3-sialylation found in MAL-II blotting and the increase of the sialylated diantennary structures assigned to GP22 detected by NP-HPLC suggest that the α 2,3-sialylation of serum proteins is increased in the course of Hashimoto's thyroiditis.

4. Discussion

Changes of protein glycosylation have been reported to be strongly associated with the progression of many types of human cancers [36] and inflammatory diseases [13]. For that reason, *N*-glycosylation is taken into consideration as a marker of different types of human disorders. The alterations of protein glycosylation profile in pathological conditions have been analyzed for cellular [37] and secreted proteins [38,39]. For clinical practice; however, it is important to look for glyco-biomarkers in fluid body samples, and analyses of human serum are currently the main focus in this field.

Glycosylation of serum proteins in Hashimoto's thyroiditis has been poorly studied so far and only IgG, as the main serum glycoprotein has been analyzed. The previous research showed that the core fucosylation of anti-Tg IgG in HT patients was lower than in Graves' disease (GD) and papillary thyroid carcinoma (PTC) donors [40] and higher than in healthy individuals [41]. The content of Man, terminal SA, and Gal β 1,4GlcNAc β 1,2Man structure in anti-Tg was also significantly elevated in HT compared to healthy control [41]. The enhanced sialylation and fucosylation of anti-Tg were correlated with the titer of this antibody in HT patients' sera [41]. Our recent research, in turn, demonstrated a decrease of IgG fucosylation in AITD patients, and we suggested that it might determine more potent antibody-dependent cell-mediated cytotoxicity (ADCC) reaction in Hashimoto's thyroid tissue (Martin et al., unpublished data). The changes of sialylation were also proved for thyroid tissue of AITD patients with the use of the following lectins: *Tritrichomonas mobilensis* lectin (TML) which recognizes SA without linkage preferences as well as SNA and MAL-II specific for α 2,6- and α 2,3-linked SA, respectively. The different MAL-II staining profile of thyroid histochemical specimens from HT, GD, and healthy donors was found. The expression of α 2,3-linked SA in follicular cells, especially in the luminal surfaces of their cell membrane, was higher in HT and GD specimens than normal thyroid gland [42].

The present study focused on the identification of altered *N*-glycan structures in HT IgG-depleted sera. We compared *N*-glycomes between HT patients and healthy control using two different strategies: the analysis of the released *N*-glycans and the study of *N*-glycosylated



Supplementary Fig. 6. Lectin analysis of fucosylation (A) and sialylation (B) in IgG-depleted serum from healthy control (C) and Hashimoto's thyroiditis (HT) after PNGase digestion. IgG-depleted serum samples (10 μ g) were de-*N*-glycosylated using PNGase (Sigma-Aldrich, P-7367) and separated by 10% SDS-PAGE under reducing conditions. (A) LCA, UEA-I and AAL were used to analysis of fucosylation. (B) SNA and MAL-II were applied to detect sialic acid-bearing glycans. Molecular masses were verified using Precision Plus Protein™ Dual Color Standards (Bio-Rad, 1610374).

serum proteins. Both approaches showed that the sialylation of *N*-glycans is altered in HT patients' serum proteins. The results indicated that the sialylated complex-type *N*-glycans with antennary Fuc are more abundant in HT serum proteins. Adding to that, the more intensive reaction with α 2,3-SA-specific MAL-II lectin in HT serum samples was observed.

On the other hand, the total sialylation of *N*-glycans was slightly reduced in HT, but this result was not statistically significant. LCA lectin staining demonstrated the reduction of α 1,6-fucosylation in HT serum glycoproteins. This decrease of serum protein core fucosylation corresponds with our previous results, which showed a reduction of core α 1,6-Fuc in IgG isolated from AITD patients (Martin et al., unpublished data). The increased level of the sialylated complex-type *N*-glycans assigned to GP22 was not accompanied by the change of the total serum sialylation. The glycosylation analysis was performed for a mixture of secreted proteins produced by different tissues. The relatively minor change of glycosylation identified by HPLC might concern only a limited number of proteins which glycosylation is regulated by the autoimmune process. Moreover, HPLC results reflect *N*-glycome profile, whereas in lectin blotting both *N*- and *O*-glycans were analyzed and for this reason, the results of the total sialylation and fucosylation differ between these two analytical approaches.

The results obtained in the present study and the literature data mentioned above show that the HT autoimmunity is accompanied by the glycosylation changes of serum proteins. Taking into consideration that the level of thyroid hormones and TSH is stable in HT patients due to levothyroxine (T4) substitution, an immune response seems to be the

most probable cause of *N*-glycosylation changes. The alterations of total plasma/serum *N*-glycosylation during an acute phase of inflammation were described previously. Reiding and co-workers observed the relationship between *N*-glycosylation of serum proteins and the clinical markers of metabolic health and inflammation in healthy individuals from the Leiden Longevity Cohort Study. A positive association between the level of high sensitivity C reactive protein (hs-CRP) and tri- and tetra-antennary *N*-glycans was identified. Furthermore, the enhanced sialylation of fucosylated di- and tri-antennary *N*-glycans has been proved to be correlated with the elevated hs-CRP level [43], which corresponds to our HPLC results obtained for GP22 in HT and the augmented α 2,3-sialylation of HT serum glycoproteins demonstrated by MAL-II blotting. The study by Reiding and co-workers indicated that the fucosylation of diantennary *N*-glycans decreased with the higher hs-CRP level, whereas the fucosylation of tri-antennary structures intensified in this inflammation process [43]. Yasukawa et al. in the mouse model of inflammation also showed that the change in concentration of acute phase proteins is accompanied by an alteration of their sialylation profile. The liver expression of *ST3Gal* and *ST6GalNAc* sialyltransferases was accelerated during inflammation and reduced to the baseline level after inflammation silencing [44].

Altered glycosylation of single serum protein has been described in autoimmune disorders. The analysis of transferrin, a negative acute phase protein, showed a difference in serum concentration of its five glycoforms in juvenile idiopathic arthritis (JIA), the most common rheumatic condition in children. Transferrin glycoforms differed in SA content between JIA and healthy subjects. The relative serum

concentration of tetrasialotransferrin was significantly lower and pentasialotransferrin significantly higher in JIA in comparison to controls [45]. The analysis of serum protein N-glycosylation after immunotherapy was performed in patients with inflammatory arthritis. Upregulation of the core-fucosylated, galactosylated diantennary structures and a decrease of the sialylated tri-antennary glycans content with and without antennary Fuc were observed after anti-TNF therapy of patients with rheumatoid arthritis and psoriatic arthritis. The authors suggested that N-glycosylation change of serum proteins is associated with silencing of inflammatory processes as the result of anti-TNF therapy [20]. The expression of glycosyltransferases, besides the availability of sugar substrate and environmental factors, is the primary regulator of oligosaccharide composition and branching. It was shown that the glycosyltransferase expression is regulated by cytokines in inflammation states [46]. Exposure to IL-6 and IL-8 resulted in the higher expression of *FUT11*, *FUT3*, *ST6Gal2*, and *ST3Gal6* in human bronchial mucosa [47]. An influence of TNF α on the expression of *FUT3*, *FUT4*, *ST3Gal3*, and *ST3Gal4* suggested the relation between chronic inflammation in cystic fibrosis and the altered glycosylation profile of human airway mucins in the course of this disease [48]. The above results prove the role of proinflammatory agents in glycosyltransferase expression. The state of chronic inflammation in HT patients might also affect the sialyltransferase expression in plasma and liver cells, the primary sources of serum proteins.

Future studies are necessary to evaluate the functional consequences of the observed sialylation changes in HT autoimmunity. Based on the literature data, we can assume that the enhanced sialylation of some serum proteins might be necessary for their interactions with sialic acid-binding immunoglobulin-like lectins (Siglecs) present on immune cells. Siglecs play a significant role in the regulation of immune system [49,50] by binding SA-containing ligands widely distributed on the host and pathogenic cells [51]. One of the members belonging to the Siglec family with proven ability to bind sialylated plasma proteins is CD22, a B-cell surface receptor. Hanasaki and co-workers showed that recombinant CD22 binds haptoglobin and IgM from human plasma and this binding is blocked by α 2,6-sialylated ligand or the sialidase treatment in case of IgM [52]. The further study revealed that CD22 interaction with IgM-antigen complex influences B-cell activation [53]. In the light of the described data and our results, it seems likely that the altered sialylation of serum/plasma proteins influences immune cell activity via interaction of these sialoproteins with Siglecs.

In conclusion, HPLC analysis of N-glycosylation of IgG-depleted serum proteins followed by LC-MS N-glycan structure identification allowed to detect the changes of serum protein sialylation in HT patients in comparison to healthy individuals. The altered sialylation has been additionally confirmed by more intensive reaction with α 2,3-SA-specific MAL-II lectin in HT serum. The present results completed our previous IgG N-glycosylation analysis in AITD patients, and both studies clearly show that the altered N-glycosylation is an evident manifestation of autoimmunity process in HT.

The following are the supplementary data related to this article.

Authors contribution

MZ performed research, analyzed data and wrote the manuscript; PLL analyzed and interpreted NP-HPLC data, prepared figures and revised manuscript; MN analyzed and interpreted LC-MS data; TM performed statistical analysis; RTJ and MTM recruited donors; EP designed and supervised research, revised manuscript and prepare figures.

Acknowledgments

This work was supported by the Jagiellonian University in Krakow grants No. K/DSC/002996, K/DSC/003987 and partially by the Polish National Science Center (grant No. 2015/18/E/NZ6/00602). The

authors have read the journal's authorship agreement and declare no conflicts of interest.

References

- [1] A. Antonelli, S.M. Ferrari, A. Corrado, A. Di Domenicantonio, P. Fallahi, Autoimmune thyroid disorders, *Autoimmun. Rev.* 14 (2015) 174–180, <https://doi.org/10.1016/j.autrev.2014.10.016>.
- [2] D.L. Mincer, I. Jialal, *Hashimoto Thyroiditis*, StatPearls Publishing, Treasure Island (FL), 2018.
- [3] Y. Tomer, D.A. Greenberg, E. Concepcion, Y. Ban, T.F. Davies, Thyroglobulin is a thyroid specific gene for the familial autoimmune thyroid diseases, *J. Clin. Endocrinol. Metab.* 87 (2002) 404–407, <https://doi.org/10.1210/jcem.87.1.8291>.
- [4] R.A. Ajjan, A.P. Weetman, The pathogenesis of Hashimoto's thyroiditis: further developments in our understanding, *Horm. Metab. Res.* 47 (2015) 702–710, <https://doi.org/10.1055/s-0035-1548832>.
- [5] S. Bliddal, C.H. Nielsen, U. Feldt-Rasmussen, Recent advances in understanding autoimmune thyroid disease: the tallest tree in the forest of polyautoimmunity, *F1000Res* 6 (2017) 1776, <https://doi.org/10.12688/f1000research.11535.1>.
- [6] B. Kristensen, L. Hegedüs, H.O. Madsen, T.J. Smith, C.H. Nielsen, Altered balance between self-reactive T helper (Th)17 cells and Th10 cells and between full-length forkhead box protein 3 (FoxP3) and FoxP3 splice variants in Hashimoto's thyroiditis, *Clin. Exp. Immunol.* 180 (2015) 58–69, <https://doi.org/10.1111/cei.12557>.
- [7] A.K. Horst, C. Wagener, Bitter sweetness of complexity, *Top. Curr. Chem.* 288 (2009) 1–15, https://doi.org/10.1007/128_2008_8.
- [8] M. Zabczyńska, K. Kozłowska, E. Pocheć, Glycosylation in the thyroid gland: vital aspects of glycoprotein function in thyrocyte physiology and thyroid disorders, *Int. J. Mol. Sci.* 19 (2018), <https://doi.org/10.3390/ijms19092792>.
- [9] A. Klein, Human total serum N-glycome, in: G.S. Makowski (Ed.), *Advances in Clinical Chemistry*, vol. 46, Academic Press, Burlington, 2008, pp. 51–85 978-0-12-374209-4 [https://doi.org/10.1016/S0065-2423\(08\)00402-2](https://doi.org/10.1016/S0065-2423(08)00402-2).
- [10] K. Biskup, E.I. Braicu, J. Sehoul, R. Tauber, V. Blanchard, The serum glycome to discriminate between early-stage epithelial ovarian cancer and benign ovarian diseases, *Dis. Markers* 2014 (2014) 238197, <https://doi.org/10.1155/2014/238197>.
- [11] S. Ozcan, D.A. Barkauskas, L. Renee Ruhaak, et al., Serum glycan signatures of gastric cancer, *Cancer Prev. Res. (Phila.)* 7 (2014) 226–235, <https://doi.org/10.1158/1940-6207>.
- [12] R. Saldova, A. Asadi Shehni, V.D. Haakensen, et al., Association of N-glycosylation with breast carcinoma and systemic features using high-resolution quantitative UPLC, *J. Proteome Res.* 13 (2014) 2314–2327, <https://doi.org/10.1021/pr401092y>.
- [13] O. Gornik, G. Lauc, Glycosylation of serum proteins in inflammatory diseases, *Dis. Markers* 25 (2008) 267–278, <https://doi.org/10.1155/2008/493289>.
- [14] E. Gindzienska-Sieskiewicz, P.A. Klimiuk, D.G. Kisiel, A. Gindzienski, S. Sierakowski, The changes in monosaccharide composition of immunoglobulin G in the course of rheumatoid arthritis, *Clin. Rheumatol.* 26 (2007) 685–690, <https://doi.org/10.1007/s10067-006-0370-7>.
- [15] F. Vučković, J. Krištić, I. Gudelj, et al., Association of systemic lupus erythematosus with decreased immunosuppressive potential of the IgG glycome, *Arthritis Rheum.* 67 (2015) 2978–2989, <https://doi.org/10.1002/art.39273>.
- [16] I. Trbojević Akmačić, N.T. Venthani, E. Theodoratou, et al., Inflammatory bowel disease associates with proinflammatory potential of the immunoglobulin G glycome, *Inflamm. Bowel Dis.* 21 (2015) 1237–1247, <https://doi.org/10.1097/MIB.0000000000000372>.
- [17] I. Gudelj, P.P. Salo, I. Trbojević-Akmačić, et al., Low galactosylation of IgG associates with higher risk for future diagnosis of rheumatoid arthritis during 10 years of follow-up, *Biochim. Biophys. Acta Mol. Basis Dis.* 1864 (2018) 2034–2039, <https://doi.org/10.1016/j.bbadis.2018.03.018>.
- [18] K. Higai, Y. Aoki, Y. Azuma, K. Matsumoto, Glycosylation of site-specific glycans of alpha1-acid glycoprotein and alterations in acute and chronic inflammation, *Biochim. Biophys. Acta* 1725 (2005) 128–135, <https://doi.org/10.1016/j.bbagen.2005.03.012>.
- [19] C. Panzironi, B. Silvestrini, M.Y. Mo, et al., An increase in the carbohydrate moiety of alpha 2-macroglobulin is associated with systemic lupus erythematosus (SLE), *Biochem. Mol. Biol. Int.* 43 (1997) 1305–1322.
- [20] E.S. Collins, M.C. Galligan, R. Saldova, et al., Glycosylation status of serum in inflammatory arthritis in response to anti-TNF treatment, *Rheumatology (Oxford)* 52 (2013) 1572–1582, <https://doi.org/10.1093/rheumatology/ket189>.
- [21] K.R. Reiding, G.C.M. Vreeker, A. Bondt, et al., Serum protein N-glycosylation changes with rheumatoid arthritis disease activity during and after pregnancy, *Front Med (Lausanne)* 4 (2018) 241, <https://doi.org/10.1074/mcp.RA117.000454>.
- [22] H. Nakagawa, M. Hato, Y. Takegawa, et al., Detection of altered N-glycan profiles in whole serum from rheumatoid arthritis patients, *J. Chromatogr. B Anal. Technol. Biomed. Life Sci.* 853 (2007) 133–137, <https://doi.org/10.1016/j.jchromb.2007.03.003>.
- [23] F. Clerc, M. Novokmet, V. Dotz, et al., Plasma N-glycan signatures are associated with features of inflammatory bowel diseases, *Gastroenterology* 155 (2018) 829–843, <https://doi.org/10.1053/j.gastro.2018.05.030>.
- [24] J.L. Stanta, R. Saldova, W.B. Struwe, et al., Identification of N-glycosylation changes in the CSF and serum in patients with schizophrenia, *J. Proteome Res.* 9 (2010) 4476–4489, <https://doi.org/10.1021/pr1002356>.
- [25] H.L. Gui, C.F. Gao, H. Wang, et al., Altered serum N-glycomics in chronic hepatitis B patients, *Liver. Int.* 30 (2010) 259–267, <https://doi.org/10.1111/j.1478-3231>.

- 2009.02170.x.
- [26] S.W. de Vroome, S. Holst, M.R. Gironde, et al., Serum N-glycome alterations in colorectal cancer associate with survival, *Oncotarget* 9 (2018) 30610–30623, <https://doi.org/10.18632/oncotarget.25753>.
- [27] R. Saldova, Y. Fan, J.M. Fitzpatrick, R.W. Watson, P.M. Rudd, Core fucosylation and alpha2-3 sialylation in serum N-glycome is significantly increased in prostate cancer comparing to benign prostate hyperplasia, *Glycobiology* 21 (2011), <https://doi.org/10.1093/glycob/cwq147> 195–05.
- [28] K. Biskup, E.I. Braicu, J. Sehouli, et al., Serum glycome profiling: a biomarker for diagnosis of ovarian cancer, *J. Proteome Res.* 12 (2013) 4056–4063, <https://doi.org/10.1021/pr400405x>.
- [29] P. Link-Lenczowski, M. Bubka, C.I.A. Balog, et al., The glycomic effect of N-acetylglucosaminyltransferase III overexpression in metastatic melanoma cells. GnT-III modifies highly branched N-glycans, *Glycoconj. J.* 35 (2018) 217–231, <https://doi.org/10.1007/s10719-018-9814-y>.
- [30] J.L. Abrahams, M.P. Campbell, N.H. Packer, Building a PGC-LC-MS N-glycan retention library and elution mapping resource, *Glycoconj. J.* 35 (2018) 15–29, <https://doi.org/10.1007/s10719-017-9793-4>.
- [31] M.P. Campbell, L. Royle, C.M. Radcliffe, R.A. Dwek, P.M. Rudd, GlycoBase and autoGU: tools for HPLC-based glycan analysis, *Bioinformatics* 24 (2008) 1214–1216, <https://doi.org/10.1093/bioinformatics/btn090>.
- [32] A.C. Russell, M. Šimurina, M.T. Garcia, et al., The N-glycosylation of immunoglobulin G as a novel biomarker of Parkinson's disease, *Glycobiology* 27 (2017) 501–510, <https://doi.org/10.1093/glycob/cwx022>.
- [33] A. Ceroni, K. Maass, H. Geyer, et al., GlycoWorkbench: a tool for the computer-assisted annotation of mass spectra of glycans, *J. Proteome Res.* 7 (2008) 1650–1659, <https://doi.org/10.1021/pr7008252>.
- [34] D. Hoja-Lukowicz, P. Link-Lenczowski, A. Carpentieri, et al., L1CAM from human melanoma carries a novel type of N-glycan with Galβ1-4Galβ1- motif. Involvement of N-linked glycans in migratory and invasive behaviour of melanoma cells, *Glycoconj. J.* 30 (2013) 205–225, <https://doi.org/10.1007/s10719-012-9374-5>.
- [35] Y. Benjamini, Y. Hochberg, Controlling the false discovery rate: a practical and powerful approach to multiple testing, *J. R. Stat. Soc. Ser. B Stat Methodol.* 57 (1995) 289–300.
- [36] J.C. de Freitas, J.A. Morgado-Díaz, The role of N-glycans in colorectal cancer progression: potential biomarkers and therapeutic applications, *Oncotarget* 7 (2016), <https://doi.org/10.18632/oncotarget.6283> 19395–13.
- [37] D. Hoja-Lukowicz, M. Przybyło, M. Duda, E. Pocheć, M. Bubka, On the trail of the glycan codes stored in cancer-related cell adhesion proteins, *Biochim. Biophys. Acta Gen. Subj.* 1861 (2017) 3237–3257, <https://doi.org/10.1016/j.bbagen.2016.08.007>.
- [38] Z. Kyselova, Y. Mechref, P. Kang, et al., Breast cancer diagnosis and prognosis through quantitative measurements of serum glycan profiles, *Clin. Chem.* 54 (2008) 1166–1175, <https://doi.org/10.1373/clinchem.2007.087148>.
- [39] G. Tabarés, C.M. Radcliffe, S. Barrabés, et al., Different glycan structures in prostate-specific antigen from prostate cancer sera in relation to seminal plasma PSA, *Glycobiology* 16 (2006) 132–145, <https://doi.org/10.1093/glycob/cwj042>.
- [40] L. Zhao, M. Liu, Y. Gao, et al., Glycosylation of sera thyroglobulin antibody in patients with thyroid diseases, *Eur. J. Endocrinol.* 168 (2013) 585–592, <https://doi.org/10.1530/EJE-12-0964>.
- [41] S. Yuan, Q. Li, Y. Zhang, et al., Changes in anti-thyroglobulin IgG glycosylation patterns in Hashimoto's thyroiditis patients, *J. Clin. Endocrinol. Metab.* 100 (2015) 717–724, <https://doi.org/10.1210/jc.2014-2921>.
- [42] P. Janega, A. Cerná, I. Kholová, E. Brabencová, P. Babál, Sialic acid expression in autoimmune thyroiditis, *Acta Histochem.* 104 (2002) 343–347, <https://doi.org/10.1078/0065-1281-00676>.
- [43] K.R. Reiding, L.R. Ruhaak, H.W. Uh, et al., Human plasma N-glycosylation as analyzed by matrix-assisted laser desorption/ionization-fourier transform ion cyclotron resonance-MS associates with markers of inflammation and metabolic health, *Mol. Cell. Proteomics* 16 (2017) 228–242, <https://doi.org/10.1074/mcp.M116.065250>.
- [44] Z. Yasukawa, C. Sato, K. Kitajima, Inflammation-dependent changes in alpha2,3-, alpha2,6-, and alpha2,8-sialic acid glycotopes on serum glycoproteins in mice, *Glycobiology* 15 (2005) 827–837, <https://doi.org/10.1093/glycob/cwi068>.
- [45] E. Gruszevska, M. Sienkiewicz, P. Abramowicz, et al., Serum profile of transferrin isoforms in juvenile idiopathic arthritis: a preliminary study, *Rheumatol. Int.* 38 (2018) 1235–1240, <https://doi.org/10.1007/s00296-018-4051-z>.
- [46] A. Grigorian, H. Mkhikian, M. Demetriou, Interleukin-2, Interleukin-7, T cell-mediated autoimmunity, and N-glycosylation, *Ann. N. Y. Acad. Sci.* 1253 (2012) 49–57, <https://doi.org/10.1111/j.1749-6632.2011.06391.x>.
- [47] S. Groux-Degroote, M.A. Krzewinski-Recchi, A. Cazet, et al., IL-6 and IL-8 increase the expression of glycosyltransferases and sulfotransferases involved in the biosynthesis of sialylated and/or sulfated Lewis x epitopes in the human bronchial mucosa, *Biochem. J.* 410 (2008) 213–223, <https://doi.org/10.1042/BJ20070958>.
- [48] P. Delmotte, S. Degroote, J.J. Lafitte, et al., Tumor necrosis factor alpha increases the expression of glycosyltransferases and sulfotransferases responsible for the biosynthesis of sialylated and/or sulfated Lewis x epitopes in the human bronchial mucosa, *J. Biol. Chem.* 277 (2002) 424–431, <https://doi.org/10.1074/jbc.M109958200>.
- [49] B.S. Bochner, N. Zimmermann, Role of siglecs and related glycan-binding proteins in immune responses and immunoregulation, *J. Allergy Clin. Immunol.* 135 (2015), <https://doi.org/10.1016/j.jaci.2014.11.031> 598–08.
- [50] P.R. Crocker, A. Varki, Siglecs, sialic acids and innate immunity, *Trends Immunol.* 22 (6) (2001) 337–342, [https://doi.org/10.1016/S1471-4906\(01\)01930-5](https://doi.org/10.1016/S1471-4906(01)01930-5).
- [51] P.R. Crocker, J.C. Paulson, A. Varki, Siglecs and their roles in the immune system, *Nat. Rev. Immunol.* 7 (2007) 255–266, <https://doi.org/10.1038/nri2056>.
- [52] K. Hanasaki, L.D. Powell, A. Varki, Binding of human plasma sialoglycoproteins by the B cell-specific lectin CD22. Selective recognition of immunoglobulin M and haptoglobin, *J. Biol. Chem.* 31 (270) (1995) 7543–7550.
- [53] T. Adachi, S. Harumiya, H. Takematsu, et al., CD22 serves as a receptor for soluble IgM, *Eur. J. Immunol.* 42 (2012) 241–247, <https://doi.org/10.1002/eji.201141899>.